

ORIGINAL ARTICLE

# Measurement of Refractive Errors in Young Myopes Using the COAS Shack-Hartmann Aberrometer

THOMAS O. SALMON, OD, PhD, FAAO, ROGER W. WEST, PhD, OD, WAYNE GASSER, OD,  
and TODD KENMORE, OD

*College of Optometry, Northeastern State University, Tahlequah, Oklahoma*

**ABSTRACT:** *Purpose.* To evaluate the Complete Ophthalmic Analysis System (COAS; WaveFront Science) for accuracy, repeatability, and instrument myopia when measuring myopic refractive errors. *Methods.* We measured the refractive errors of 20 myopic subjects (+0.25 to -10 D sphere; 0 to -1.75 D cylinder) with a COAS, a phoropter, and a Nidek ARK-2000 autorefractor. Measurements were made for right and left eyes, with and without cycloplegia, and data were analyzed for large and small pupils. We used the phoropter refraction as our estimate of the true refractive error, so accuracy was defined as the difference between phoropter refraction and that of the COAS and autorefractor. Differences and means were computed using power vectors, and accuracy was summarized in terms of mean vector and mean spherocylindrical power errors. To assess repeatability, we computed the mean vector deviation for each of five measurements from the mean power vector and computed a coefficient of repeatability. Instrument myopia was defined as the difference between cycloplegic and noncycloplegic refractions for the same eyes. *Results.* Without cycloplegia, both the COAS and autorefractor had mean power vector errors of 0.3 to 0.4 D. Cycloplegia improved autorefractor accuracy by 0.1 D, but COAS accuracy remained the same. For large pupils, COAS accuracy was best when Zernike mode  $Z_4^0$  (primary spherical aberration) was included in the computation of sphere power. COAS repeatability was slightly better than autorefractor repeatability. Mean instrument myopia for the COAS was not significantly different from zero. *Conclusions.* When measuring myopes, COAS accuracy, repeatability, and instrument myopia were similar to those of the autorefractor. Error margins for both were better than the accuracy of subjective refraction. We conclude that in addition to its capability to measure higher-order aberrations, the COAS can be used as a reliable, accurate autorefractor. (*Optom Vis Sci* 2003;80:6-14)

Key Words: wavefront, aberration, aberrometer, Shack-Hartmann, automated refraction, accuracy, repeatability, instrument myopia, refractive error

Aberrometers, also known as wavefront sensors, are instruments that scientists have been using for over 10 years to study the monochromatic aberrations of the human eye.<sup>1, 2</sup> These instruments have provided valuable new information about the eye's optics,<sup>3-10</sup> and how aberrations change with age,<sup>11</sup> with accommodation,<sup>12</sup> after refractive surgery,<sup>13, 14</sup> and with keratoconus, cataracts, and tear film anomalies.<sup>15</sup>

The *total* aberrations measured by a wavefront sensor include higher-order aberrations as well as the lower-order aberrations, referred to by refractionists as spherical and cylindrical refractive errors. Until recently, when determining refractive error, clinicians generally ignored higher-order aberrations. This was because, for most patients, they had little effect on vision and were too difficult

to measure and correct. Recently, however, the clinical measurement of higher-order aberrations has become important for patient care, especially for refractive surgery cases. When conventional refractive surgeries correct sphere and cylinder, they often create unnatural higher-order aberrations that can degrade vision, especially with large pupils. To improve optical and visual results, the new generation of refractive lasers will rely on aberrometers to guide their ablations. More doctors will also begin using clinical aberrometers for pre- and postoperative evaluation of refractive surgery patients as well as for other problems associated with the optics of the eye.

Among the different types of wavefront sensors, Shack-Hartmann-based devices have become the most popular. Early research

with laboratory-built Shack-Hartmann sensors indicates that they can measure aberrations in both model and living eyes with great accuracy. One of the first *clinical* Shack-Hartman aberrometers, the Complete Ophthalmic Analysis System (COAS, manufactured by WaveFront Sciences) became available in late 2000. As shown in Fig. 1, the COAS is similar to an autorefractor in size and appearance. Like an autorefractor, the patient positions his head on a chin rest and fixates the center of a circular grid, which is optically fogged by about 1.5 D. The operator manually aligns a reference box on a video monitor with the pupil and then takes a single or multiple measurements with one click of a button. After alignment and a preliminary estimate of the refractive error, each wavefront measurement takes 1/30 second. The aberrometer uses an array of square lenslets that measure the wavefront aberration in the pupil at 210- $\mu\text{m}$  intervals. This allows approximately 600 sample points within a 6.0-mm-diameter pupil and provides very high resolution sampling of the aberrations. The high sampling and close spacing of the lenslets allows the COAS to measure large aberrations, including spherical refractive errors between  $-15$  D myopia and  $+7$  D hyperopia and astigmatism up to 6 D. It can measure pupil diameters between 3.5 and 9.0 mm. The light source used for measurement is an 840-nm infrared super luminescent diode, and results are converted to a user-selected wavelength (default setting 550 nm). After each measurement, the attached computer displays a color map of both the total and higher-order wavefront aberration, along with a numerical list showing the spherocylindrical refractive error to the nearest 0.01 D (corneal or spectacle plane; plus- or minus-cylinder format), pupil size to the nearest 0.1 mm, total and higher-order root mean square wavefront error, peak-to-valley wavefront errors, and Zernike coefficients (Malacara<sup>16</sup> or Optical Society of America<sup>17</sup> format) from the third order up to 12th order. If the user selects the “Seidel sphere” option, the spherical power is based on a computation that includes primary spher-



**FIGURE 1.** The current version of the Complete Ophthalmic Analysis Systems (COAS). It is similar to an autorefractor in size and operation.

ical aberration. The COAS records these data, as well as the lower-order Zernike coefficients to a database, and provides other display options, including a three-dimensional, animated wavefront map and simulation of the patient’s view of a 20/200 Snellen letter with or without correction for selected aberrations.

Until recently, aberrometers were largely confined to research laboratories, but new clinical instruments, such as the COAS, are providing clinicians with the ability to routinely measure aberrations of their patients. Because COAS measurements include the lower-order aberrations of sphere and cylinder, we were interested in determining how well it measures these refractive errors. That is, in addition to providing higher-order aberration data, can it also be used as a common autorefractor? We investigated this by testing its accuracy, repeatability, and instrument myopia when measuring the refractive errors of young myopes.

## METHODS

Subjects were 20 volunteers between the ages of 18 and 35 years. All had healthy eyes with refractive errors between  $+0.25$  and  $-10.00$  D sphere and 0 to  $-1.75$  D cylinder. We obtained institutional review board approval and informed consent from each subject before collecting data. We measured the refractive errors of both right and left eyes in dim illumination using three methods: (1) COAS wavefront sensor, (2) Nidek ARK-2000 autorefractor, and (3) phoropter. All eyes were measured first without, then with cycloplegia (2 drops, 1% cyclopentolate). For each eye and condition, we took five COAS, five autorefractor, and two phoropter refraction measurements (independently repeated by two clinicians). Because the COAS objectively measures pupil size to the nearest 0.1 mm, we also used its data to estimate pupil sizes for phoropter measurements, which were completed shortly before the COAS measurements. All COAS measurements were made for the full pupil, but for the purposes of analysis, we computed refractive errors for both large and small pupils. Large pupil analysis was based on the full pupil, which varied for each eye and measurement (mean diameter of 6.7 mm without and 7.7 mm with cycloplegia). For the small pupil analysis, we recomputed the wavefront aberration and refractive errors for a reduced pupil size of 4.0 mm for all eyes. The Nidek autorefractor measures a fixed zone with a diameter of approximately 3.5 mm in the central pupil. By default, the COAS uses only Zernike mode  $Z_2^0$  (defocus) to compute the spherical equivalent power, but if the user chooses the “Seidel sphere” option, it will incorporate mode  $Z_4^0$  (primary spherical aberration) into the computation. We processed COAS data for each eye using both the default and Seidel sphere setting.

## COAS Computation of Spherocylindrical Refractive Error

The COAS measures the eye’s wavefront aberration function based on the Shack-Hartmann principle.<sup>1, 2</sup> The raw data consist of a set of Zernike coefficients that quantify the type and magnitude of aberrations present. Zernike polynomials are used to systematically organize optical aberrations into modes, each of which represents an optical aberration with a specific form.<sup>17, 18</sup> Modes are grouped into orders, and the second Zernike order contains

three modes, designated  $Z_2^{-2}$  (45/135 astigmatism),  $Z_2^0$  (defocus), and  $Z_2^2$  (90/180 astigmatism). The respective coefficients for these modes,  $C_2^{-2}$ ,  $C_2^0$ , and  $C_2^2$  may be used to compute the spherocylindrical refractive error in the following steps.

1. Correct the Zernike coefficients for chromatic aberration. The initial set of Zernike coefficients are based on a wavefront measured with 840-nm infrared light, so this must be corrected to the appropriate value for a user-specified wavelength, which is set to 550 nm by default. All Zernike coefficients, except  $C_2^0$  (defocus), are adjusted according to Equation 1, where  ${}^\lambda C_n^m$  is the coefficient for the selected wavelength,  ${}^{840}C_n^m$  is the original coefficient,  $n_\lambda$  is the index of refraction for water at the selected wavelength, and  $n_{840}$  is the index of refraction for water at 840 nm.

$${}^\lambda C_n^m = \left( \frac{n_\lambda - 1}{n_{840} - 1} \right)^{840} C_n^m \quad (1)$$

The refractive index values for  $n_\lambda$  and  $n_{840}$  can be found by Equation 2,<sup>19</sup> where the wavelength ( $\lambda$ ) is written in nanometers.

$$n_\lambda = 1.320535 - \frac{4.685}{(\lambda - 214.102)} \quad (2)$$

2. Convert Zernike coefficients to power vectors. As an intermediate step, the coefficients are converted to a refractive power vector of the form  $[J_{45}, M, J_{180}]$ . The components  $J_{45}$ ,  $M$ , and  $J_{180}$ , respectively, represent the power of a Jackson crossed-cylinder with axes at 45 and 135°, the spherical equivalent power, and the power of a Jackson crossed-cylinder with axes at 180 and 90°. If the coefficients are expressed in meters and  $y$  is the pupil radius in meters, Equations 3 to 5 compute the refractive power in diopters for each vector component.<sup>9</sup>

$$J_{45} = (-2\sqrt{6}/y^2)C_2^{-2} \quad (3)$$

$$M = (-4\sqrt{3}/y^2)C_2^0 \quad (4)$$

$$J_{180} = (-2\sqrt{6}/y^2)C_2^2 \quad (5)$$

3. Correct the spherical equivalent for wavelength. The COAS adjusts the spherical equivalent power ( $M$ ) for chromatic aberration because the measurement is made using 840-nm infrared light but is reported for visible light (550 nm by default). The formula (Equation 6) also assumes that the infrared light is reflected from a plane 0.125 mm (expressed in meters for  $X$  in Equation 6) posterior to the retina of a 60 D model eye, which has a focal length in air of 16.667 mm (expressed in meters for  $L$  in Equation 6). This is necessary because the subjective focal plane will be at the level of the photoreceptors, perhaps the external limiting membrane,<sup>20</sup> but the infrared light used for measurement passes through to deeper layers and is predominantly reflected from within the choroid.<sup>21</sup> Variable  $M$  in Equation 6 represents the new spherical equivalent power corrected for wavelength  $\lambda$ .

$$M = 60 - \left[ \frac{1}{(L + X)} - M_{840} \right] \left( \frac{n_\lambda - 1}{n_{840} - 1} \right) \quad (6)$$

4. Calculate the Seidel sphere. If the user selects the Seidel sphere option, the COAS will add the value  $M_s$ , computed in Equation 7, to the value of  $M$  computed in Equation 4. Because the  $Z_2^0$  term is a parabola, inclusion of the  $Z_4^0$  term (primary spherical aberration) should, in theory, improve the fit of the wavefront to a sphere and improve accuracy of the spherical equivalent power. Note that according to this formula, a positive spherical aberration (positive  $C_4^0$  coefficient) adds a small amount of positive dioptric power, which will decrease a myopic prescription.

$$M_s = (12\sqrt{5}/y^2)C_4^0 \quad (7)$$

5. Compute sphere, cylinder, and axis. Use Equations 8 to 10 and the pseudo code below to convert  $J_{45}$ ,  $M$  (or  $M_s$ ), and  $J_{180}$  to sphere, cylinder, and axis of the clinical minus-cylinder notation.<sup>9</sup> (Note that reference 9 contains a typographical error in the last line of pseudo code at the bottom of page 668. It is correctly written as the second line of pseudo code after Equa-

**TABLE 1.**

Refraction accuracy for noncycloplegic Complete Ophthalmic Analysis System (COAS) and autorefractor (AR) measurements<sup>a</sup>

	Pupil Diameter (mm)	OD				OS			
		Vector	Sphere	Cylinder	Axis	Vector	Sphere	Cylinder	Axis
COAS	4.0	+0.30 ± 0.04	-0.04 ± 0.10	-0.15 ± 0.06	168	+0.35 ± 0.05	+0.04 ± 0.11	-0.25 ± 0.06	177
	6.7 <sup>b</sup>	+0.33 ± 0.03	0.15 ± 0.11	-0.16 ± 0.08	171	+0.41 ± 0.05	+0.23 ± 0.13	-0.29 ± 0.08	179
AR	3.5	+0.33 ± 0.07	-0.01 ± 0.13	-0.20 ± 0.08	173	+0.34 ± 0.05	-0.02 ± 0.11	-0.20 ± 0.07	179

<sup>a</sup> Results show the mean difference from phoropter refraction for 20 right and 20 left eyes. Intervals show standard errors. Mean differences are displayed in terms of mean power vector magnitude and mean sphere-cylinder-axis power difference from phoropter refraction. Negative values for the sphere indicate that the instrument measured more myopia than the phoropter refraction; positive values indicate more hyperopia. COAS results for a uniform 4-mm-diameter pupil for all subjects are based on the default (non-Seidel) computation of sphere power. Accuracy with the Seidel algorithm for a 4-mm pupil diameter (not shown) was the same or only marginally worse. COAS full-pupil (mean diameter, 6.7 mm) results were based on the Seidel computation of sphere power because it was slightly more accurate than the default sphere (not shown). Vector, sphere, and cylinder units are in diopters. Axes are in degrees.

<sup>b</sup> Maximum pupil diameter, which varied with each eye and measurement. The mean noncycloplegic pupil diameter was 6.7 ± 0.7 mm (SD) with a range of 5.3 to 8.0 mm for OD and 4.3 to 7.7 mm for OS.

tion 10.) For plus-cylinder notation, change the negative sign in Equation 8 to positive and use Equations 9 and 10 as written.

$$\text{cylinder} = -2\sqrt{J_{45}^2 + J_{180}^2} \tag{8}$$

$$\text{sphere} = M - \text{cylinder}/2 \tag{9}$$

$$\text{axis} = \frac{1}{2} \tan^{-1}\left(\frac{J_{45}}{J_{180}}\right) \tag{10}$$

After computing Equation 10, modify the axis value according to the Excel pseudo code below to ensure that the minus-cylinder axis is a value between 0 and 180°.

IF (J<sub>180</sub> = 0, IF (J<sub>45</sub><0, 135, 45), IF (J<sub>180</sub><0, axis + 90, IF (J<sub>45</sub>≤0, axis + 180, axis))).

For the plus-cylinder axis, reverse the direction of all three inequality signs, as shown below.

IF (J<sub>180</sub> = 0, IF (J<sub>45</sub>>0, 135, 45), IF (J<sub>180</sub>>0, axis + 90, IF (J<sub>45</sub>≥0, axis + 180, axis))).

### Accuracy

Accuracy (statistical validity) describes how well an instrument measures what it is designed to measure. The COAS measures both higher- and lower-order aberrations, but for this study, we limited our assessment to the lower-order aberrations of sphere and cylinder.

We had no absolute “gold standard” for the *true* refractive error with which to compare the COAS data, so we used the clinical subjective refraction as the best estimate because it is presently considered the most reliable technique for establishing a spectacle prescription. In selecting this standard, we were mindful that individual subjective refractions are accurate to only about ±0.25 D for both sphere and cylinder. Although a subjective optometer might have been used to estimate the true refractive error, we had greater confidence in the accuracy of standard clinical phoropter refraction. Data used to assess accuracy were processed in the following steps.

1. Each COAS, Nidek autorefractor, and subjective phoropter measurement was converted to a power vector with the form [J<sub>45</sub>, M, J<sub>180</sub>]. Each of these represents an independent power

profile that can be summed to equal the original spherocylindrical prescription.<sup>22</sup>

2. The vector mean of each set of five COAS and Nidek autorefractor measurements and two subjective phoropter refractions were computed. Subsequent steps are described specifically for the COAS data but were also followed for the Nidek autorefractor data.
3. Estimated COAS error (vector E) for each eye was defined as the difference between the mean COAS (vector C) and subjective phoropter refraction vector ( $\vec{S}$ ) as shown in Equation 11:

$$\vec{E} = \vec{C} - \vec{S} \tag{11}$$

4. Overall COAS accuracy was taken as the mean of the COAS error vectors, averaged across the 20 eyes in each testing condition (cycloplegic, noncycloplegic, right, left, large pupil, small pupil, Seidel, and non-Seidel). The mean error vector was converted back to clinical sphere, cylinder, and axis to simplify interpretation. We computed the Hotelling T<sup>2</sup> statistic and equivalent F statistic to test the null hypothesis that the value of the mean error vector was not significantly different from zero.<sup>23, 24</sup>
5. We also computed the magnitude (m) of the COAS error vector (vector E, above) for each eye according to Equation 12 where J<sub>45</sub>, M and J<sub>180</sub> were components of vector E. This can be interpreted as the absolute dioptric error, in vector space, of each eye’s COAS measurement.<sup>25</sup> We then computed the mean magnitude of these errors across 20 eyes, tested under the various conditions.

$$m = \sqrt{J_{45}^2 + M^2 + J_{180}^2} \tag{12}$$

### Repeatability

Repeatability (statistical reliability) describes how consistent successive measurements are. For each eye and condition (noncycloplegic and cycloplegic), five measurements with the COAS were taken within a few minutes of each other. We processed the data and analyzed repeatability according to the steps outlined below. These steps were used to process COAS data with both the default and Seidel sphere and for both large and small pupils. Autorefractor repeatability was computed in the same manner.

1. Each COAS measurement was converted to power vector form.
2. The mean COAS vector was computed, and then the vector

**TABLE 2.** Cycloplegic refraction accuracy for the Complete Ophthalmic Analysis System (COAS) and autorefractor (AR)<sup>a</sup>

	Pupil Diameter (mm)	OD				OS			
		Vector	Sphere	Cylinder	Axis	Vector	Sphere	Cylinder	Axis
COAS	4.0	+0.31 ± 0.04	+0.03 ± 0.10	-0.19 ± 0.05	1	+0.33 ± 0.05	+0.10 ± 0.11	-0.18 ± 0.06	170
	7.7 <sup>b</sup>	+0.38 ± 0.04	+0.14 ± 0.12	-0.13 ± 0.08	7	+0.43 ± 0.06	+0.23 ± 0.14	-0.17 ± 0.08	171
AR	3.5	+0.21 ± 0.03	+0.14 ± 0.07	-0.18 ± 0.06	4	+0.23 ± 0.03	+0.18 ± 0.07	-0.15 ± 0.05	161

<sup>a</sup> Data are arranged and formatted similarly to that in Table 1.

<sup>b</sup> Maximum pupil diameter, which varied with each eye and measurement. The mean cycloplegic pupil diameter was 7.7 ± 0.4 mm (SD) with a range of 6.6 to 8.4 mm for OD and 6.4 to 8.4 mm for OS.

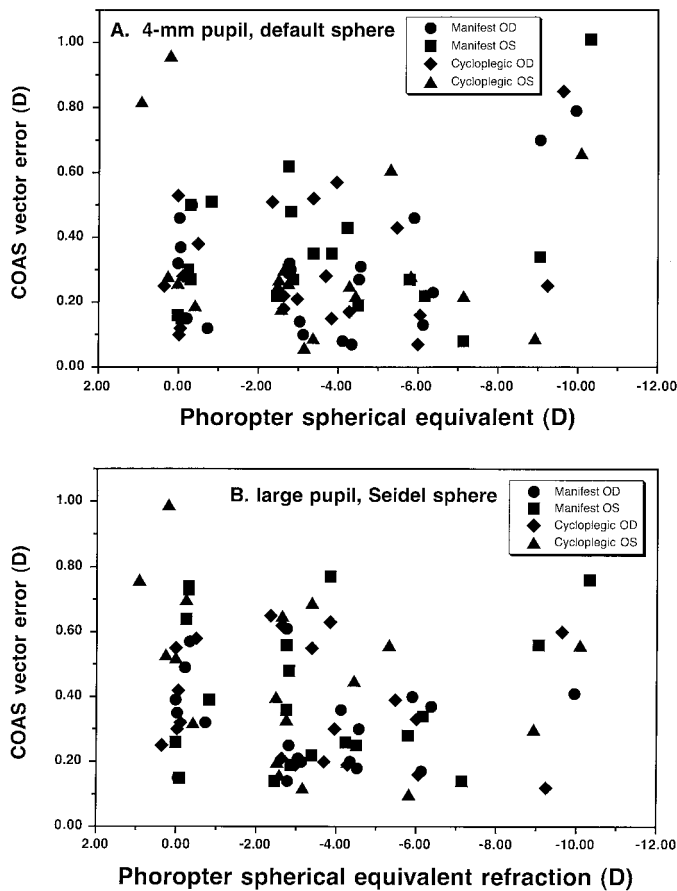


**FIGURE 2.** Complete Ophthalmic Analysis Systems (COAS) accuracy for small and large pupils. Distribution of COAS power vector errors as a function of phoropter spherical equivalent refraction for right and left eyes, with and without cycloplegia. A: data points are based on a uniform 4.0-mm-diameter pupil and the default COAS algorithm for computing sphere because it gave marginally less error than the Seidel algorithm. B: data points are based the maximum pupil size for each measurement using the Seidel algorithm because it was slightly more accurate than the default algorithm. Mean  $\pm$  SD of pupil diameters were  $6.7 \pm 0.7$  mm without cycloplegia and  $7.7 \pm 0.4$  mm with cycloplegia. See Tables 1 and 2 for summary statistics.

difference of each of the five measurements from the mean was computed. We referred to this as the vector deviation from the mean for each of the five measurements.

3. We computed the magnitude of each deviation vector (Equa-

**TABLE 3.**

Repeatability coefficients for the Complete Ophthalmic Analysis System (COAS) (4.0 mm and full pupil) and autorefractor, in diopters, for right and left eyes with and without cycloplegia<sup>a</sup>

Condition	Eye	COAS (4-mm)	COAS (Full Pupil)	Autorefractor
Manifest	OD	0.30	0.26	0.29
	OS	0.24	0.22	0.32
Cycloplegia	OD	0.15	0.13	0.18
	OS	0.16	0.11	0.19

<sup>a</sup> Results shown here were computed using the default (non-Seidel) sphere because the Seidel results were marginally worse and similar to the autorefractor values.

tion 12), then computed the mean deviation (mean of five magnitudes) for each eye.

4. We squared and summed the mean deviations for the 20 eyes in each group, then divided by 20 to obtain the root mean squared deviation.
5. Finally we computed a repeatability coefficient, defined as the root mean square deviation multiplied by 1.96.

This analysis generally follows the methods described by Bland and Altman<sup>26</sup> and used in other studies of repeatability for clinical refraction.<sup>27–29</sup> Those studies tested repeatability in terms of power differences for one meridian only, but to use the complete power vector, we substituted the deviation vector for their differences. Our repeatability coefficient corresponds to their 95% limit of agreement.

### Instrument Myopia

Instrument myopia is a source of error in tabletop instruments that measure refractive errors, because many patients accommodate while viewing internal fixation targets that are optically projected to infinity. This causes the instrument to overestimate myopia or underestimate hyperopia. We computed instrument myopia for the COAS and the Nidek autorefractor in the following steps. Although these steps are described for the COAS data they were identically followed for the Nidek autorefractor data.

1. Cycloplegia could have induced a slight change in the actual refractive error, so for each eye, we computed any such change (vector  $\Delta$ ) as the difference between the *subjective* noncycloplegic (vector  $S_m$ ) and *subjective* cycloplegic (vector  $S_c$ ) power vectors (Equation 13).

$$\vec{\Delta} = \vec{S}_m - \vec{S}_c \tag{13}$$

2. Instrument myopia (vector  $I$  in Equation 14) for each eye was defined as the difference between the COAS noncycloplegic (vector  $C_m$ ) and COAS cycloplegic (vector  $C_c$ ) refractions minus the true change (vector  $\Delta$ , from Equation 13).

$$\vec{I} = \vec{C}_m - \vec{C}_c - \vec{\Delta} \tag{14}$$

The mean of all right-eye COAS instrument myopia values was computed and a similar analysis was performed for left eyes. We also computed instrument myopia separately for the different test conditions of large and small pupils and with the default or Seidel

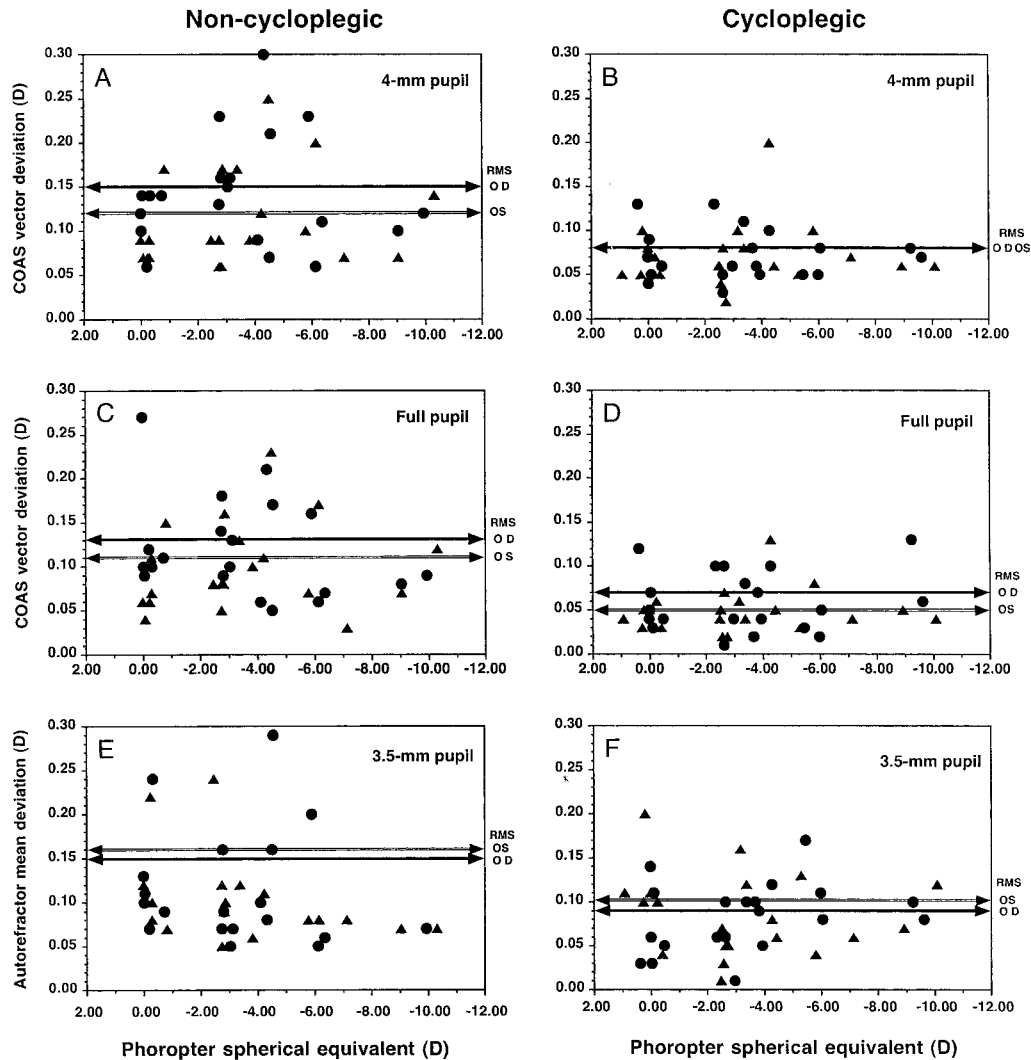


**FIGURE 3.**

Complete Ophthalmic Analysis Systems (COAS) and autorefractor repeatability. Each data point shows the mean power vector deviation from the mean power vector, computed from five repeated measurements for each eye. Results are plotted as a function of phoropter spherical equivalent refraction. All COAS results are based on the default (not Seidel) algorithm for computing the sphere because it showed better repeatability. The top row (A, B) shows results for a 4.0-mm-diameter pupil. The middle row (C, D) shows results based on the maximum pupil for each measurement (mean  $\pm$  SD, 6.7  $\pm$  0.7 mm without cycloplegia and 7.7  $\pm$  0.4 mm with cycloplegia). The bottom row (D, E) shows results for the autorefractor (pupil diameter, 3.5 mm). The left column shows results without cycloplegia, and the right column shows results with cycloplegia. Filled circles indicate OD data, and the filled horizontal arrows show the root mean square (RMS) vector deviations for OD. Filled triangles indicate OS data, and the open horizontal arrow shows the RMS vector deviations for OS. See Table 3 for summary statistics.

sphere. Mean instrument myopia power vectors were converted to sphere, cylinder and axis and the mean spherical equivalent power was also recorded.

## RESULTS

### Accuracy

Table 1 summarizes accuracy of noncycloplegic refractions for the COAS and autorefractor in terms of the mean power vector error, and the mean sphere-cylinder-axis error for right and left eyes, and for the different pupil sizes. Means and standard errors (N = 20) are shown. Power vector errors are shown in bold because they best show the mean departure of each instrument's measurement from the subjective refraction with a single number. For right eyes, COAS small and large pupil and autorefractor mean vector

error were about 0.3 D. Left-eye errors were marginally worse, approximately 0.4 D.

Interpretation of the sphere-cylinder-axis error is less obvious because it represents the mean of twenty spherocylindrical power differences between the COAS, or autorefractor and the phoropter refraction. As such, the sphere, cylinder and axis should not be viewed as three separate scalar quantities but as a single vector. The sign of the spherical power indicates the power error, for the COAS or autorefractor, in the meridian of the axis (close to 180° in all cases). A negative sign indicates that the instrument measured too much minus; a positive sign indicates too much plus, relative to the phoropter refraction. Meanwhile, because all the axes were oriented horizontally, these instruments tended to measure excess negative power, in the

amounts shown in the cylinder column, in the vertical meridians.

COAS 4.0-mm pupil accuracy data were based on refractions using the default sphere because accuracy with the Seidel sphere was the same or marginally worse. COAS full-pupil measurements were based on refractions using the Seidel sphere because, for large pupils, these data were most accurate.

Table 2 likewise summarizes accuracy statistics for cycloplegic refractions. COAS large and small pupil accuracies were similar to that shown in Table 1. The autorefractor showed about a 0.1 D improvement in accuracy with cycloplegia. In all cases, except one (COAS, OS, full pupil, Seidel sphere;  $p = 0.18$ ) mean COAS and autorefractor measurements showed statistically significant differences from subjective refractions by the Hotelling  $T^2$  test ( $p \leq 0.05$ ), which allows multivariate analysis of power vectors as a whole.<sup>23</sup> For all COAS test conditions and combinations, the spherical equivalent accounted for 84 to 91% of the error, whereas astigmatism accounted for the remainder of the variance between COAS and subjective refractions.<sup>24</sup> The mean sphere and cylinder errors for both COAS (large and small pupils) and autorefractor, shown in Tables 1 and 2 were less than about  $\pm 0.25$  D, which is within the clinical accuracy of subjective refraction under ideal conditions.

Fig. 2A shows the distribution of COAS vector errors, as a function of phoropter spherical equivalent refraction for a uniform 4.0-mm diameter pupil (default sphere). Most of the power vector errors (83%) were within 0.50 D of zero diopters. There was no apparent correlation between COAS error and magnitude of the spherical equivalent refractive error. Fig. 2B shows a similar analysis for the full pupil diameter, which varied from eye to eye and measurement to measurement, but had a mean value of 7.7 mm with cycloplegia and 6.7 mm without. With the full pupil, errors were slightly greater, but still small in terms of clinical accuracy, because 84% of the power vector errors were  $< 0.60$  D. For both Fig. 2A and B, the most extreme errors were about 1.00 D. For comparison, 91% of the autorefractor vector errors were  $< 0.50$  D, but its most extreme error was about 1.60 D.

## Repeatability

Repeatability for the COAS (4-mm and full pupil) and autorefractor is summarized in Table 3, which shows the repeatability coefficients, in diopters, for right and left eyes with and without cycloplegia. COAS repeatability for the 4-mm and full pupil was slightly better when the default COAS sphere was used, therefore only those data are listed. For most cases, repeatability with the COAS was slightly better than the autorefractor. Without cycloplegia it was about 0.25 D or better; with cycloplegia it improved to about 0.15 D. Repeatability with the Seidel algorithm was slightly worse and similar to that of the autorefractor.

Fig. 3 presents repeatability, in terms of the mean deviations (refer to Methods), as a function of phoropter spherical equivalent refraction. This is similar to the difference vs. mean plots recommended by Bland and Altman<sup>26</sup> and used by Zadnik et al.<sup>29</sup> Each of the six graphs include results for right and left eyes and are organized with noncycloplegic refractions in the left columns (Fig. 3 A, C, and E) and cycloplegic refraction in the right column (Fig. 3 B, D, and F). The top pair of graphs (Fig. 3 A and B) show results

for the COAS analyzed for a 4-mm-diameter pupil and using the default sphere. The middle pair (Fig. 3 C and D) are for the COAS with full-pupil data, also with the default sphere, and the bottom pair (Fig. 3 E and F) are for autorefraction. The horizontal arrows indicate the level of the root mean square deviation for right and left eyes on each graph. For both COAS pupil sizes and the autorefractor, the use of cycloplegia improved repeatability. The smaller spread of points for the COAS shows that its repeatability was slightly better than the autorefractor, especially with cycloplegia (Fig. 3 B and D). Among noncycloplegic COAS refractions, the largest deviations were for medium myopes ( $-2.00$  to  $-6.00$  D). With cycloplegia, there appeared to be relatively constant level of COAS repeatability across the entire spherical equivalent refractive error range.

## Instrument Myopia

Table 4 summarizes instrument myopia for the COAS and Nidek autorefractor in terms of the spherical equivalent change in refraction. COAS results listed are for the full pupil using the default sphere, but instrument myopia was essentially the same for 4-mm pupils and with the Seidel sphere. Results are shown in diopters with  $\pm 1$  SEM. The COAS showed less spherical equivalent instrument myopia than the autorefractor—essentially no instrument myopia. For both the right- and left-eye COAS and right-eye autorefractor measurements, instrument myopia was not statistically significantly different from zero (Hotelling  $T^2$  test;  $p < 0.05$ ).

## DISCUSSION

We found that the COAS has a range of accuracy similar to both clinical subjective refraction and Nidek autorefraction under noncycloplegic and cycloplegic conditions. The mean COAS, autorefraction, and subjective phoropter refractions showed statistically significant differences from each other, however the differences were smaller than the accuracy with which we can measure subjective refraction (approximately  $\pm 0.25$  D). Therefore, we could not rule out the possibility that either the COAS or the autorefractor was more accurate than subjective refraction for measuring lower-order aberrations.

**TABLE 4.** Mean instrument myopia for the Complete Ophthalmic Analysis System (COAS) and autorefractor, expressed as the spherical equivalent power, in diopters ( $\pm 1$  SEM)<sup>a</sup>

Eye	COAS	Autorefractor
OD	$-0.01 \pm 0.07$	$-0.16 \pm 0.10$
OS	$-0.05 \pm 0.07$	$-0.23 \pm 0.08$

<sup>a</sup> A negative value indicates that the noncycloplegic refraction was more myopic than the cycloplegic refraction. A small change in astigmatic power, about 0.1 D (not shown), accompanied the instrument myopia for both the COAS and autorefractor. COAS results are for full pupil (mean, 7.7 mm), non-Seidel computations of refractive error. Instrument myopia for the COAS was approximately the same when analyzed for 4-mm-diameter pupils and with the Seidel algorithm.

Analysis of variability showed that 80 to 90% of the COAS/subjective discrepancy was due to differences in the spherical equivalent powers. Several factors could have accounted for this. (1) Dioptric compensation for the depth of the COAS fundus reflection, presumably from the choroid, might not exactly match the subjective best focus. This is further complicated by the fact that the layer of reflectance varies from person to person and depends on factors such as the amount of melanin or hemoglobin present at that site.<sup>30</sup> (2) Subjective refractions were performed with incandescent light, but the COAS refracts with 850-nm infrared light, then it mathematically corrects this for a default value of 550 nm at the peak of the visible spectrum to allow for the effects of chromatic aberration. Because the subjective examination was done with a letter chart projected by an incandescent light bulb, a more accurate comparison should be gained by setting the wavelength correction to about 570 nm. This should allow a shift in COAS spherical measurements by about  $-0.1$  D.<sup>31</sup> (3) Slight differences and fluctuations in pupil size and state of accommodation between the time we measured the phoropter and the COAS refractions might have contributed to small differences in the non-cycloplegic refractions. A change in pupil size would affect primary spherical and higher-order aberrations, but probably more important, it would affect the depth of focus for the eye, smaller pupil diameters giving an increased depth of field,<sup>32, 33</sup> and consequently greater variability in measured refractive error. (4) Subjective best focus might balance total aberrations, whereas the default COAS spherical equivalent (non-Seidel) is based on a single mode,  $Z_2^0$  (defocus) and the Seidel sphere added compensation for  $Z_4^0$  (primary spherical aberration). This is consistent with our observation that the Seidel sphere improved accuracy by about 0.1 D (mean power vector), but for large pupils only.

In most cases, repeatability for the COAS was slightly better than the Nidek autorefractor. Repeatability improved with cycloplegia but was slightly worse when the Seidel option was used, with or without cycloplegia. Finally, there was no significant instrument myopia with the COAS.

For the measurement of lower-order aberrations (sphere and astigmatism) accuracy, repeatability, and instrument myopia with the COAS were good enough that it should serve as a reliable autorefractor. As we learn how to better compensate for factors affecting the spherical equivalent power, it might be possible to refine accuracy even further. Our study was limited to an assessment of lower-order aberrations, and these results cannot be extrapolated to higher-order terms. The manufacturer of the COAS, WaveFront Sciences, tested accuracy with phase plates and found errors of  $<0.05$   $\mu\text{m}$  in the value of fourth-order and other Zernike coefficients. Their repeatability studies with a human eye found a standard deviation ( $N = 30$ ) for third- and fourth-order Zernike coefficients of  $<0.05$   $\mu\text{m}$ .

Wavefront sensors such as the COAS allow the measurement of the full complement of higher- plus lower-order aberrations, which has become important in clinical practice, especially for doctors who manage refractive surgery patients. These aberrometers can also be used for the early diagnosis of keratoconus, cataracts, and tear film anomalies<sup>15</sup> and may assist in the evaluation of other apparently healthy, nonamblyopic eyes that cannot be corrected to 20/20 with spectacles. Aberrometers can also help us objectively evaluate and improve the optical design of contact lenses.<sup>34</sup> In a

separate study, we have been comparing the optical performance of an aspheric soft contact lens, designed to correct spherical aberration, with that of a conventional spherical lens.<sup>34</sup> Aberrometry has revolutionized visual optics research and will certainly make an increasingly important contribution to clinical eye care in the coming years.

## ACKNOWLEDGMENTS

We thank the Northeastern State University Faculty Research Council for providing a faculty research grant to T. Salmon and R. West and WaveFront Sciences for providing a travel grant to T. Salmon. Preliminary results of this research were presented as a poster at the American Academy of Optometry annual meeting in Philadelphia, PA in December 2001; a revised poster was presented at the Third International Congress on Wavefront Sensing and Aberration-free Refractive Correction in Interlaken, Switzerland in February 2002.

Received April 3, 2002; revision received September 30, 2002.

## REFERENCES

- Liang J, Grimm B, Goetz S, Bille JF. Objective measurement of wave aberrations of the human eye with the use of a Hartmann-Shack wave-front sensor. *J Opt Soc Am (A)* 1994;11:1949–57.
- Salmon TO, Thibos LN, Bradley A. Comparison of the eye's wavefront aberration measured psychophysically and with the Shack-Hartmann wave-front sensor. *J Opt Soc Am (A)* 1998;15:2457–65.
- Liang J, Williams DR. Aberrations and retinal image quality of the normal human eye. *J Opt Soc Am (A)* 1997;14:2873–83.
- Liang J, Williams DR, Miller DT. Supernormal vision and high-resolution retinal imaging through adaptive optics. *J Opt Soc Am (A)* 1997;14:2884–92.
- Prieto PM, Vargas-Martin F, Goetz S, Artal P. Analysis of the performance of the Hartmann-Shack sensor in the human eye. *J Opt Soc Am (A)* 2000;17:1388–98.
- Hofer H, Artal P, Singer B, Aragon JL, Williams DR. Dynamics of the eye's wave aberration. *J Opt Soc Am (A)* 2001;18:497–506.
- Moreno-Barriuso E, Marcos S, Navarro R, Burns SA. Comparing laser ray tracing, the spatially resolved refractometer, and the Hartmann-Shack sensor to measure the ocular wave aberration. *Optom Vis Sci* 2001;78:152–6.
- Marcos S, Diaz-Santana L, Llorente L, Dainty C. Ocular aberrations with ray tracing and Shack-Hartmann wave-front sensors: does polarization play a role? *J Opt Soc Am (A)* 2002;19:1063–72.
- Salmon TO, Thibos LN. Videokeratoscope-line-of-sight misalignment and its effect on measurements of corneal and internal ocular aberrations. *J Opt Soc Am (A) Opt Image Sci Vis* 2002;19:657–69.
- Thibos L, Hong X, Bradley A, Cheng X. Statistical variation of aberration structure and image quality in a normal population of healthy eyes. *J Opt Soc Am (A)* 2002;19:2329–47.
- Artal P, Berrio E, Guirao A, Piers P. Contribution of the cornea and internal surfaces to the change of ocular aberrations with age. *J Opt Soc Am (A)* 2002;19:137–43.
- Pallikaris LG, Panagopoulou SI, Siganos CS, Molebny VV. Objective measurement of wavefront aberrations with and without accommodation. *J Refract Surg* 2001;17:S602–7.
- Hong X, Thibos LN. Longitudinal evaluation of optical aberrations following laser *in situ* keratomileusis surgery. *J Refract Surg* 2000;16:S647–50.
- Marcos S. Refractive surgery and optical aberrations. *Optics Photonics News* 2001; No.1:22–5.
- Thibos LN, Hong X. Clinical applications of the Shack-Hartmann aberrometer. *Optom Vis Sci* 1999;76:817–25.

16. Malacara D. *Optical Shop Testing*, 2nd ed. New York: Wiley, 1992.
17. Thibos LN, Applegate RA, Schwiegerling JT, Webb R. Standards for reporting the optical aberrations of eyes. In: Lakshminarayanan V, ed. *Trends in Optics and Photonics. Vision Science and Its Applications*, Vol 35. OSA Technical Digest Series. Washington, DC: Optical Society of America, 2000:232–44.
18. Atchison D, Scott D, Cox M. Mathematical treatment of ocular aberrations: a user's guide. In: Lakshminarayanan V, ed. *Trends in Optics and Photonics. Vision Science and Its Applications*, Vol 35. OSA Technical Digest Series. Washington, DC: Optical Society of America, 2000:110–30.
19. Thibos LN, Ye M, Zhang XX, Bradley A. The chromatic eye: a new reduced-eye model of ocular chromatic aberration in humans. *Appl Optics* 1992;31:3594–600.
20. Williams DR, Brainard DH, McMahon MJ, Navarro R. Double-pass and interferometric measures of the optical quality of the eye. *J Opt Soc Am (A)* 1994;11:3123–35.
21. Elsner AE, Burns SA, Weiter JJ, Delori FC. Infrared imaging of sub-retinal structures in the human ocular fundus. *Vision Res* 1996; 36:191–205.
22. Thibos LN, Wheeler W, Horner D. Power vectors: an application of Fourier analysis to the description and statistical analysis of refractive error. *Optom Vis Sci* 1997;74:367–75.
23. Johnson RA, Wichern DW. *Applied Multivariate Statistical Analysis*. Englewood Cliffs, NJ: Prentice Hall, 1992.
24. Naeser K, Hjortdal J. Multivariate analysis of refractive data: mathematics and statistics of spherocylinders. *J Cataract Refract Surg* 2001; 27:129–42.
25. Thibos LN, Horner D. Power vector analysis of the optical outcome of refractive surgery. *J Cataract Refract Surg* 2001;27:80–5.
26. Bland JM, Altman DG. Statistical methods for assessing agreement between two methods of clinical measurement. *Lancet* 1986;1: 307–10.
27. Rosenfield M, Chiu NN. Repeatability of subjective and objective refraction. *Optom Vis Sci* 1995;72:577–9.
28. Walline JJ, Kinney KA, Zadnik K, Mutti DO. Repeatability and validity of astigmatism measurements. *J Refract Surg* 1999;15: 23–31.
29. Zadnik K, Mutti DO, Adams AJ. The repeatability of measurement of the ocular components. *Invest Ophthalmol Vis Sci* 1992;33: 2325–33.
30. Delori FC, Pflibsen KP. Spectral reflectance of the human ocular fundus. *Appl Optics* 1989;28:1061–77.
31. Bennett AG, Rabetts RB. *Bennett and Rabetts' Clinical Visual Optics*, 3rd ed. Boston: Butterworth-Heinemann, 1998.
32. Atchison DA, Charman WN, Woods RL. Subjective depth-of-focus of the eye. *Optom Vis Sci* 1997;74:511–20.
33. Campbell R. The depth of field of the human eye. *Optica Acta* 1957; 4:157–64.
34. Huffman K, Ross S, Pack L, Salmon T. Visual and optical performance of Frequency 55 aspheric vs. spheric contact lenses. *Optom Vis Sci* 2002;79:129.

**Thomas O. Salmon**  
*College of Optometry*  
*Northeastern State University*  
*1001 N. Grand Avenue*  
*Tablequah, OK 74464-7017*  
*e-mail: salmon@ipa.net*